

Article

An Energy-Efficient Start-Up Strategy for Large Variable Speed Hydro Pump Turbine Equipped with Doubly Fed Asynchronous Machine

Rassiah Raja Singh ¹, Manickavel Baranidharan ¹, Umashankar Subramaniam ², Mahajan Sagar Bhaskar ², Shriram S. Rangarajan ^{3,4}, Hany A. Abdelsalam ⁵, Edward Randolph Collins ^{4,*} and Tomonobu Senjyu ⁶

- ¹ Advanced Drives Laboratory, Department of Energy and Power Electronics, Vellore Institute of Technology, Vellore 632014, India; rrajasingh@gmail.com (R.R.S.); baranidharan.eee@gmail.com (M.B.)
- ² Renewable Energy Laboratory, College of Engineering, Prince Sultan University, Riyadh 11586, Saudi Arabia; usubramaniam@psu.edu.sa (U.S.); sagar25.mahajan@gmail.com (M.S.B.)
- ³ Department of Electrical and Electronics Engineering, SR University, Warangal 506001, India; shriras@g.clemson.edu
- ⁴ Department of Electrical and Computer Engineering, Clemson University, Clemson, SC 29634, USA
- ⁵ Department of Electrical Engineering, Kafrelsheikh University, Kafr El-Sheikh 33516, Egypt; hanyahmed2008@yahoo.com
- ⁶ Department of Electrical and Electronics Engineering, University of the Ryukyus, Nishihara 903-0213, Okinawa, Japan; b985542@tec.u-ryukyu.ac.jp
- * Correspondence: collins@clemson.edu



Citation: Singh, R.R.; Baranidharan, M.; Subramaniam, U.; Bhaskar, M.S.; Rangarajan, S.S.; Abdelsalam, H.A.; Collins, E.R.; Senjyu, T. An Energy-Efficient Start-Up Strategy for Large Variable Speed Hydro Pump Turbine Equipped with Doubly Fed Asynchronous Machine. *Energies* **2022**, *15*, 3138. <https://doi.org/10.3390/en15093138>

Academic Editor: Ferdinanda Ponci

Received: 20 February 2022

Accepted: 22 April 2022

Published: 25 April 2022

Publisher's Note: MDPI stays neutral with regard to jurisdictional claims in published maps and institutional affiliations.



Copyright: © 2022 by the authors. Licensee MDPI, Basel, Switzerland. This article is an open access article distributed under the terms and conditions of the Creative Commons Attribution (CC BY) license (<https://creativecommons.org/licenses/by/4.0/>).

Abstract: The use of a Doubly Fed Asynchronous Machine (DFAM) provides attractive characteristics and offers operational flexibility in many variable speed generation applications, such as in a hydroelectric pumped storage plant. In a variable speed hydroelectric pumped storage plant, the start-up process of DFAM is identical to the conventional singly fed asynchronous machine, wherein a significant amount of energy is wasted. This paper introduces an energy-efficient start-up strategy in DFAM based hydroelectric pump-turbine. The back-to-back voltage source converter connected to the rotor side is amenable for speed control (real power), braking (regenerative/dynamic), and starting the unit. Further, in this starting technique, the stator circuit of the machine is injected with a low voltage DC supply at starting instead of short-circuiting the windings. This DC injection reduces the slip losses and cuts down the magnetizing current requirement. The magnitude of the required DC supply is estimated based on the machine's reactive power requirement. Also, the switching of stator winding between the short circuit connection, DC injection, and grid supply is carried out using a changeover switch and determined by the speed of the rotor. The proposed starting strategy is investigated with 250 MW DFAM in Matlab/Simulink environment and experimented with a 2.2 kW DFAM prototype. Test results show that the proposed starting method can conserve more than 26.1 percent of electrical energy in the example application compared to the conventional V/f start-up strategy.

Keywords: doubly-fed asynchronous machine; DFAM; hydroelectric pumped storage plant; V/f start-up strategy; energy efficient start-up; DC injection; smooth starting

1. Introduction

The smart grid enhances the overall operation of the power system by accepting the distributed intermittent generation such as micro-hydro, the photovoltaic, wind, etc. Among the challenges confronting the integration of these generators into the grid are (i) advanced mechanisms are required to maintain high energy efficiency, reliability, and power quality, and (ii) backup storage may be needed due to intermittency. The storage system is important to balance the variations in demand for energy. Several energy storage technologies are available, including flywheel, superconducting magnetics, batteries,

pumped hydroelectric storage, and compressed air. Among these, pumped hydroelectric storage dominates for large capacity [1]. Around 140 GW of fixed speed pumped storage power plants (PSPP) are under operation throughout the world [2].

Initially, the PSPP was employed with the fixed speed in the early decades of the 20th century, where synchronous generators were started in pumping mode with the help of pony motors [3]. The fixed speed PSPP employing synchronous machines has disadvantages in terms of system efficiency, which is impacted because of: (i) change in water head level throughout the year in dam, (ii) change in excess power availability in the grid for pumping mode, and (iii) change in power generation according to grid demand for generating mode. The advancement of hydroelectric PSPP laid the path for developing a Variable Speed Pumped Storage Power Plant (VSPSP) wherein the speed of the turbine is adjusted by the water head to yield maximum efficiency and a variable speed generator is used [4]. In 1993, Japan-based Hitachi Mitsubishi Hydro Corporation started to commission the first large-rated VSPSP of 400 MW with the help of a cycloconverter to meet slip power requirements ($\pm 8.3\%$) [5,6]. In this application, a Doubly Fed Asynchronous Machine (DFAM) is used. In the pumping mode, starting of the pump-turbine is carried out by an additional static frequency converter due to the limitation of cycloconverter operation (below 16.66 Hz). (The DFAM is sometimes called a Doubly-Fed Induction Generator, or DFIG, when the asynchronous (induction) machine is used as a generator).

The advancement in power semiconductor devices in the mid-2000's caused keen interest towards the employment of 2-level back-to-back converter topologies to meet the slip power demand. In a DFAM, the V/f start-up strategy is adapted for smooth starting and is enabled through the machine side converter. Once the machine reaches the rated speed, flux-oriented vector control is enabled to control the speed and power factor with high dynamic characteristics [7]. The excitation circuit based on a 2-level voltage source converter suffers from high harmonics switching stress and needs a filter circuit in RSC (419.5 MVA Frades II) [8,9]. To overcome these practical challenges, Europe-based companies started commissioning 3-level neutral point clamped voltage source converters for the rotor excitation circuit (280 MVA Linth Limmern) [10].

In the V/f starting method, the voltage and frequency ramp from low-end to the rated value by regulating the flux constant and increasing the torque gradually. In addition to this, the speed of the machine can be accelerated as per the user's requirement using V/f starting [11]. V/f starting is devised to overcome the problems such as torque pulsations, high inrush current, and heating of the machine which is common in other starting methods. This method is extensively used in all large-rated DFAM based variable speed pumped storage plants. During start-up, the torque is produced through electromagnetic induction where the slip is the key factor [12,13]. Similarly, the current in short-circuited stator winding depends upon slip frequency and airgap flux, which is directly proportional to the rotor current. Therefore, energy consumption during start-up depends upon slip power and starting duration [14,15]. It is found that a significant quantity of energy is dissipated due to slip [16]. The slip increases the magnitude of current feeding into the motor to achieve its desired output, which causes vulnerability to the machine windings. There are two significant consequences of the slip: (1) it increases the consumption of energy and (2) it results in overheating due in the coils. These can cause early failure and more losses in the electric motor [17].

The focus of the paper is to minimize the power consumption of a DFAM during the start-up process. To conserve energy by reducing slip and magnetizing current, and effective start-up strategy is developed and implemented in DFAM. This method applies a low voltage DC supply to stator windings instead of short-circuiting, which regulates the reactive power and eliminates the slip losses. Hence, the rated torque is developed with zero slip, i.e., no slip-related losses are produced during the electromagnetic interaction between the windings. This zero-slip ramping is executed when the rotor starts to rotate at around 25% of synchronous speed and continues till the machine is synchronized with the grid. The developed energy-efficient start-up strategy is modeled and simulated in

Matlab/Simulink software and experimentally validated with a 2.2 kW DFAM. Based on simulation results, economic analysis for using this technique on a 250 MW hydrogenating unit is carried out, and it is found that the proposed system can save more than 26% of electrical energy relative to a conventional V/f start-up strategy for this application. The technique is not limited to pump-storage hydro plants, but also other systems incorporating DFAM generators.

2. Conventional Start-Up Strategy of DFAM

Figure 1 depicts the components and the connection of the DFAM system. The voltage source converter connected between rotor terminals of the machine and DC-link is known as Machine Side Converter (MSC). Similarly, the voltage source converter connected between the main supply and DC-link is known as Grid Side Converter (GSC) [18,19]. The DC-link acts as a storage element and decouples GSC and MSC in a back-to-back power converter set.

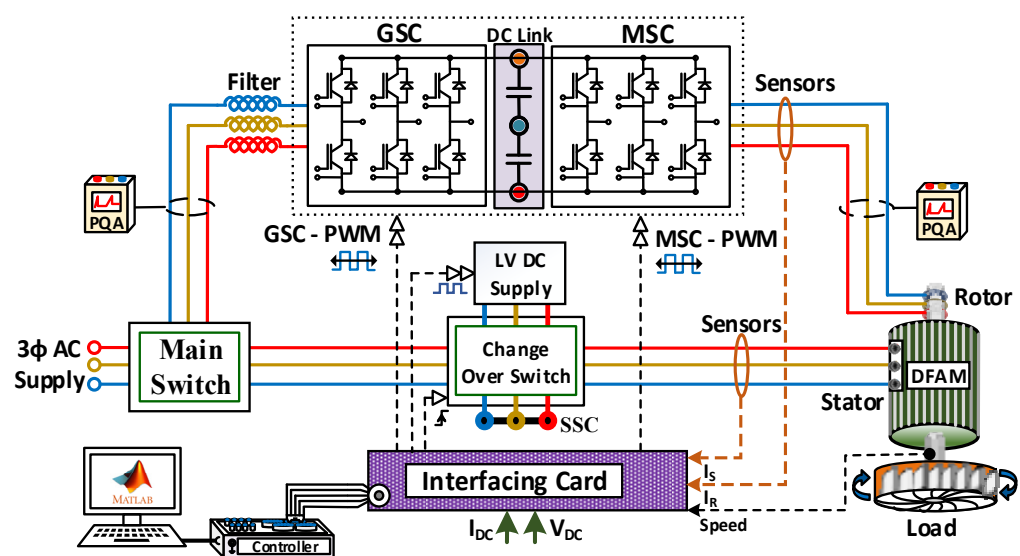


Figure 1. Schematic diagram of DFAM based PSPP system.

The DC-link supplies the required reactive power to the machine through rotor terminals. The DC-link capacity enhances the system's overall system performance [13]. Detailed control strategy with d-q modelling and control equations of GSC, MSC, and DC-link is presented in [20,21]. Compared with the traditional voltage-ramp starting method, the V/f starting method has various advantages such as simple control, faster response in starting time, low starting current, etc. During starting, GSC and MSC regulate DC-link voltage and provide a V/f ramp to supply rotor circuit current, respectively. Once the starting of DFAM is accomplished, a vector control strategy is adopted in MSC for controlling the speed and machine reactive power. The V/f starting method includes three main factors, the slope of the ramp, V/f ratio, and an initial "boost" voltage. The slope of the ramp determines starting time while considering rotor current and energy consumption, the starting period selection is essential [11]. Similarly, the V/f ratio determines the starting flux of the machine. A Simulink model of V/f starting is briefly discussed in [13]. The boost voltage is provided for developing the initial torque that overcomes the static torque and shortens start-up time. The value of the boost voltage is based on the rating of machine and rotor parameters, usually 20 to 50 percent of the rated voltage. In the course of starting, the electromagnetic torque (T_{st_e}) is derived as,

$$F_{st} = \frac{T_{st}}{T_r}(F_r), T_{max} = \left(\frac{V_r}{F_r}\right)^2 = \varphi_r, T_{st_e} = -\frac{3}{2}P_n \frac{L_m^2}{L_r} i_{dr} i_{qr} \quad (1)$$

The stator windings are switched between the short circuit terminal and grid terminal using the transfer changeover switch in a conventional start-up strategy. The changeover switch unit consists of two circuit breakers (Main and SSC) and the operation of circuit breakers is based on the signal received from the controller. A high signal closes the switch and a low signal opens the switch, and also it is ensured that only one switch may be operated at a time. The switching logic is shown in Figure 2a. The steps involved in the conventional start-up strategy of DFAM are given below.

- *Step 1 (Initiate the start-up process):* Stator short circuit (SSC) circuit breaker is closed, and the V/f ramp pulses (Scalar) are provided to the machine side rotor converter until the machine reaches the synchronous speed.
- *Step 2:* Once the machine reaches the rated speed, the V/f ramp pulses are disabled, and the SSC circuit breaker is opened.
- *Step 3 (Synchronization):* Pulses are re-enabled for adjusting machine parameters such as voltage amplitude, frequency, and phase angle of stator terminals.
- *Step 4:* Once the machine parameters are lined up with grid parameters, the main switch is closed, and the vector control strategy is adopted.

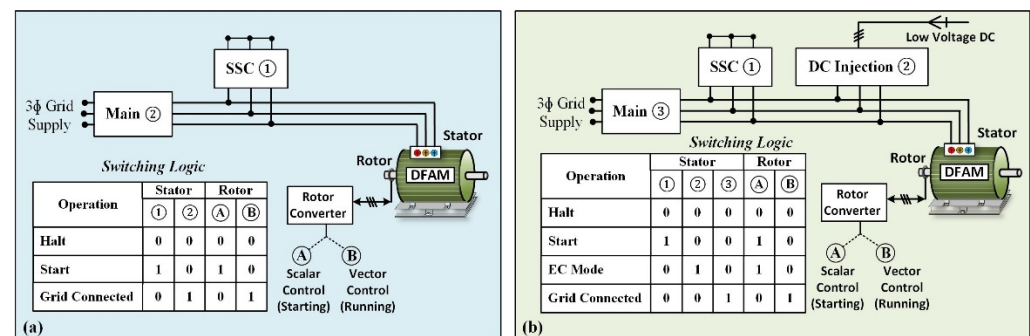


Figure 2. Connection diagram of changeover switch with switching. (a) Conventional Startup, (b) Proposed DC injection Startup.

3. Energy Efficient Start-Up Strategy

During starting, the total current drawn by the machine depends on the reactive component current (magnetization), the torque component current (acceleration), and the stator equivalent current (slip frequency) [22]. In the conventional starting method, all these currents are supplied from rotor converters that reduce the system's overall efficiency. The energy conservation (EC) start-up strategy presented in this paper is designed to reduce no-load losses and slip losses during starting by injecting a low voltage DC signal in the stator windings. Applied properly, this low voltage DC injection provides the required reactive power and eliminates the slip losses.

The DFAM system with the proposed energy-efficient DC injection start-up strategy is shown in Figures 1 and 2b. Similar to the conventional start-up, the energy-efficient DC injection start-up strategy consists of two control sections, grid side converter (GSC) control and machine side converter (MSC) control. The grid side controller regulates DC-link voltage and grid side reactive power [23]. Likewise, the machine side controller increases voltage and frequency with an aspect ratio (V/f ratio) up to the machine's rated value. Control signals from the controller are provided to the changeover switch for switching the stator winding connection from the short circuit connection, DC supply, and grid supply, as well as switching pulses to GSC and MSC. The changeover switching unit consists of three circuit breakers (Main, SSC, and DC injection), and the operation of circuit breakers is based on the signal received from the controller. A high signal closes and a low signal opens the breakers and ensures that only one switch can be operated at a time. The switching logic is shown in Figure 2b. The EC start-up strategy, switching sequence, selection of transition point, and selection of DC voltage are the subjects discussed in the subsequent sessions.

3.1. Operational Sequence of the Proposed Strategy

The implementation of an energy-efficient DC injection start-up strategy in the DFAM system is carried out through a systematic procedure, shown in Figure 3. The DC-link of the back-to-back voltage source converter is energized using a grid side converter before initiating the start-up. Once the DC-link voltage is regulated, the V/f ramp pulses are provided to the rotor converter for initiating smooth start-up “Position A—open-loop scalar control”. This operation is similar to the conventional starting approach of a DFAM. As soon as the speed of the rotor reaches 25 percent of its rate (where the rotor swing is curtailed), a low voltage DC supply is injected by switching the stator winding connection from a short circuit to a DC injection. During this period, the rotor speed matches with synchronous speed due to the elimination of slip losses. Finally, the stator windings are isolated from DC voltage and synchronized with the grid once the speed of the rotor reaches above its synchronous speed.

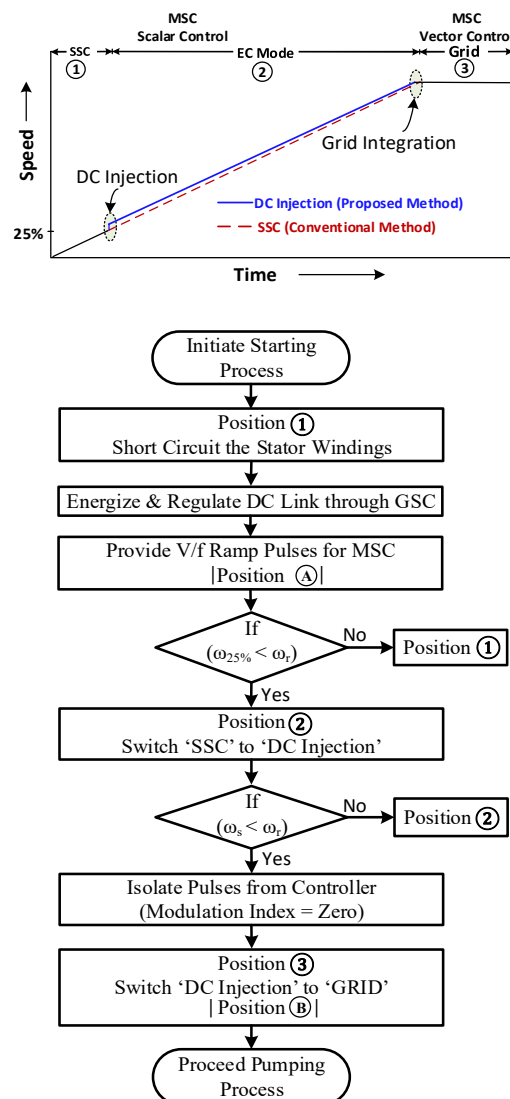


Figure 3. Operation sequence of energy efficient start-up strategy.

During this transition period, the pulses to the rotor converters are controlled to match the machine parameters such as voltage amplitude, frequency, and phase angle of stator terminals with grid parameters for synchronization. Once the machine is synchronized with the grid, the vector control strategy is adopted in MSC “Position B—closed-loop vector control”. The operational sequence of the proposed energy-efficient dc injection start-up

strategy is shown in Figure 2b. Stator winding connections are switched using circuit breakers during the starting process, whereas the switching of scalar control mode and vector control mode is carried out through a soft-switching mode. The steps involved in the energy-efficient dc injection start-up strategy of the DFAM are given below.

- *Step 1 (Initiate the start-up process):* Stator short circuit (SSC) circuit breaker is closed, and the V/f ramp pulses (Scalar) are provided to the machine side rotor converter until the machine reaches 25 percent of synchronous speed.
- *Step 2 (Energy Conservation):* At 25 percent of synchronous speed, the SSC circuit breaker is opened, and the DC injection circuit breaker is closed.
- *Step 3:* Once the machine reaches the synchronous speed, the V/f ramp pulses are disabled, and the DC injection circuit breaker is opened.
- *Step 4 (Synchronization):* Pulses are re-enabled for adjusting machine parameters such as voltage amplitude, frequency, and phase angle of stator terminals.
- *Step 5:* Once the machine parameters are lined up with grid parameters, the main switch is closed, and the vector control strategy is adopted.

3.2. Selection of Transition Point (SSC to DC Injection)

Energy is conserved through switching the stator winding of the doubly-fed asynchronous machine from SSC to DC injection. During this transition, it is mandatory to ensure the rotor and stator flux magnitude swing should be within an acceptable limit so it will not produce undesirable electromagnetic torque and power disturbances to the machine and grid [23]. As per the speed-torque characteristics of the induction motor, as shown in Figure 4 [NEMA Std.], it is shown that the pull-up acceleration takes place after 20 percent of synchronous speed. Also, as stated by Allen-Bradley, the changes in machine acceleration take place between 25 percent and 40 percent [24,25]. Through Matlab simulation, the speed-torque characteristics of a DFAM are analyzed with a conventional V/f start-up strategy. The result shows that the machine produces high electromagnetic torque at the initial stage of starting and stabilizes after the machine's acceleration. Further, it is noticed that the current and flux component of the machine is also stabilized after the acceleration. Therefore, it is decided to inject the DC voltage supply into the stator circuit after the stabilization of electromagnetic torque. This could reduce pulsations in speed and torque. Also, it is noted that the stabilizing point varies with respect to the start-up duration, power rating, and moment of inertia of the machine.

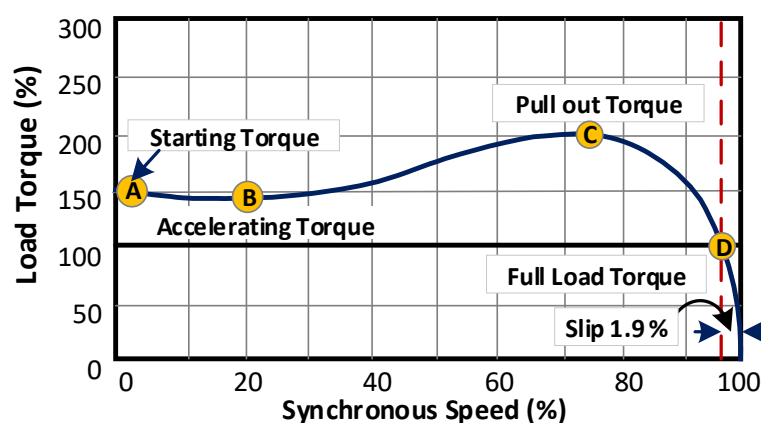


Figure 4. Operating characteristics of the asynchronous motor.

3.3. Selection of DC Voltage

The magnitude of DC voltage depends on the transient characteristics of the DFAM. Usually, to avoid oscillations, the DC supply is injected into high voltage winding [26]. Also, starting or switching current should not exceed the converter rating, but the torque should be sufficient to drive. The DC voltage is selected in consideration of performance-

related parameters, i.e., the stator and rotor currents of the DFAM should not exceed the nameplate ratings. The dynamic limit of stator and rotor current is clarified through (2) and (3) respectively.

$$I_s \geq \frac{1}{\sqrt{2}} I_{s(\text{rated_ac})} \tag{2}$$

$$I_r \geq \sqrt{\left(-\frac{L_s}{L_m} I_s \sin \delta\right)^2 + \left(\frac{\tau_{dc}}{L_m I_s \sin \delta} - \frac{L_s}{L_m} I_s\right)^2} \tag{3}$$

where, $\tau_{dc} = I_s \psi_{sdc} \sin \delta$. The DC voltage is applied at no-load conditions; therefore, the machine does not produce as many transients as compared to loaded conditions. During conventional starting, the magnetic flux of the machine is maintained by d-axis rotor current only. With a DFAM, the machine is associated with both rotor and stator d-axis currents as per (4). Further, any one of the d-axis currents (either d-axis stator current or d-axis rotor current) is enough to provide the required magnetic flux of the machine [27,28].

$$\left\{ \begin{array}{l} \vec{\psi}_{dr} = \sigma L_r \vec{I}_{dr} + \frac{L_m}{L_s} \vec{\psi}_{ds} \\ \vec{\psi}_{ds} = L_s \vec{I}_{ds} + L_m \vec{I}_{dr} \end{array} \right\} \tag{4}$$

The technique provided in this paper creates the required magnetic flux by d-axis stator current from the DC supply. The magnitude of the DC voltage is estimated based on the requirement of reactive component current during starting (no-load) and also no-load torque is considered. The estimation of reactive component current (I_{dr}) is calculated from the rotor current of the machine by Clarke and Park transformations. The DC voltage connected to the stator circuit is estimated by $V_{DC} = I_{DC} \sqrt{3} R_s / Ph$, $I_{DC} \cong I_{dr} \cong I_s$. Alternatively, the DC voltage can be estimated based on stabilization characteristics of the 2.2 kW DFAM test machine and 250 MW DFAM, as shown in Figure 5a,b, respectively. The stabilization characteristics are plotted between DC injection voltage and reactive current components. The selected DC voltage value (in case 250 MW DFAM, 2500/25 V, 4000 A) is injected to DFAM through rotor slip rings from a low voltage DC source to reduce the slip losses and provide the required reactive power for the start-up.

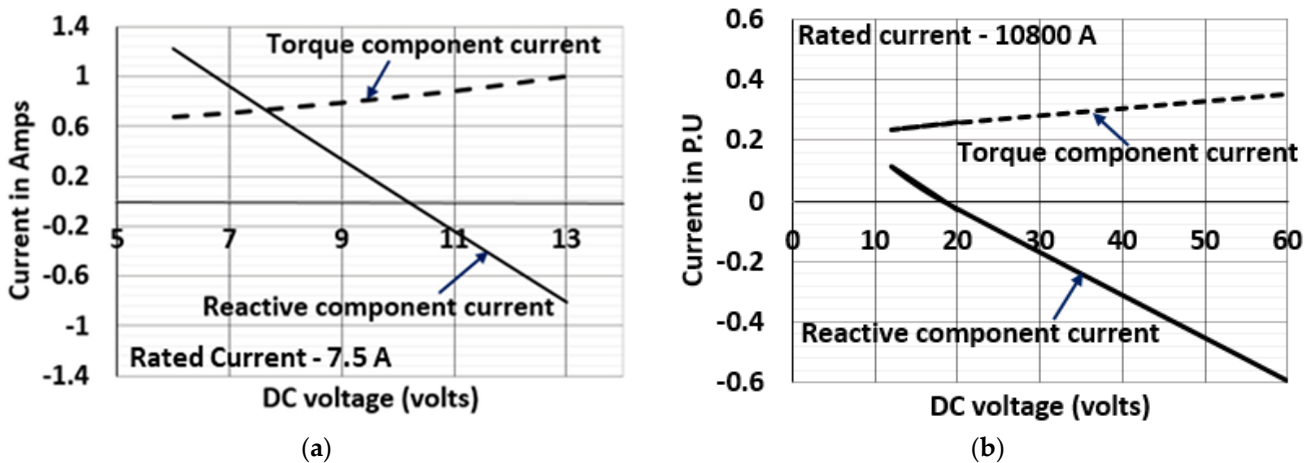


Figure 5. Stabilization characteristics, (a) 2.2 kW DFAM, (b) 250 MW DFAM.

3.4. Energy Efficient DC Injection Start-Up Strategy

The realization of the proposed energy efficient start-up strategy is carried out using the experimental arrangement depicted in Figure 6. The hardware setup consists of a 2.2 kW DFAM coupled with a dynamometer loading arrangement. A two-level IGBT based back-to-back voltage source converter (GSC and MSC) with a DC-link filter is connected between the grid and rotor terminals of the machine. The GSC controls the grid’s reactive power and maintains the DC-link voltage constant (325 V). The MSC also provides variable voltage variable frequency

supply to the rotor windings and controls the machine's reactive power. A low voltage DC supply is connected to the stator winding during an energy-efficient start-up.

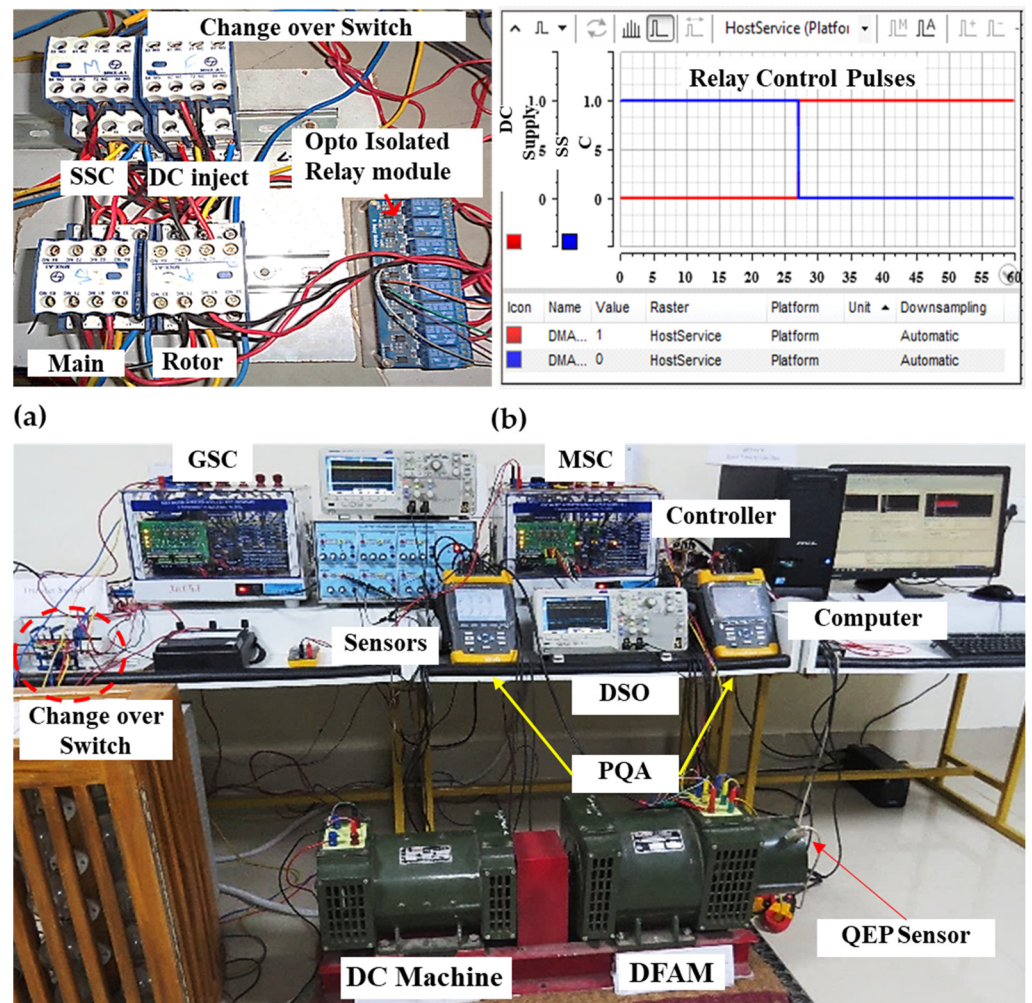


Figure 6. Snapshot of experimental arrangement. (a) Change over switch, (b) Control panel.

The following alterations to the machine were made to execute the intended research. The manual spring balance dial and the frames are removed, a load-cell arrangement is built for torque measurement. Similarly for speed measurement, the tachogenerator is replaced with a quadrature encoder pulse (QEP) sensor. A quadrature encoder pulse (QEP—Avago HEDS 5645-113) sensor is connected to the shaft for providing the pulses to the controller (512 pulses/revolution) with respect to speed and position. To control the voltage source converter and changeover switch, a real-time controller (TMS320F240 DSP) interfaced with Matlab/Simulink software is used. The Optocoupler circuit is used to isolate and intensify all the signals from the controller. To sense the voltage and current signals, Hall Effect voltage and current sensors (LV-25 P & LTS 25 NP) with an active filtering circuit are employed in the circuit. Also, the changeover switching unit consists of three 3-pole contactors with an auxiliary switch (L&T MNX 32 and MNX A1) for switching the stator windings between SSC, DC injection, and main grid supply. An additional breaker is also employed to alternately isolate or connect the rotor windings from MSC. All the breakers are controlled through optoisolated relay units (SRD-5V-SL-C, 10A). The electrical input quantities of rotor and stator are measured and recorded through three-phase power quality analyzers (PQA—Fluke 435) and dSPACE control desk 3.7.3 automation. The recorded results are analyzed using Fluke view and Power log software. A snapshot of

the experimental arrangement is depicted in Figure 6. The rating of the test machine is tabularized in Table A1 (Appendix A).

4. Result and Discussion

To perform the energy efficient start-up, the DFAM is simulated in Matlab/Simulink software and experimentally validated with 2.2 kW DFAM with a 2-level voltage source back-to-back converter. The duration of energy-efficient start-up simulation is for 5 + 1 s (5 s ramping + 1 s no load) to analyze the dynamic behaviour of the machine, especially the input current. The simulation is carried out in a 3.40 GHz i7 core central processing unit with switching frequencies of 1650 Hz for both GSC and RSC. The DC-link voltage of the 2-level back-to-back voltage source converter is maintained at 325 V by the grid side converter control system. The machine is started by energizing the rotor with a V/f ramp supply, i.e., the voltage and frequency are ramped together from initiation to rated value by regulating the flux constant which increases the speed gradually.

4.1. Simulation Results of 2.2 kW DFAM

The initial voltage and frequency are chosen as 36 volts and 2 Hz, respectively. Also, the voltage frequency (V/f) ratio is chosen as 3.7. During smooth starting, the phase-locked loop control (PLL) is used to estimate the machine's rotor angle from variable voltage variable frequency ramp supply (VVVF). The rotor current is sensed for calculating the torque component current and magnetization current using Clarke and Park transformations, which are calculated as 0.65 A (I_{qr}) and 2.784 A (I_{dr}), respectively. Estimation of DC supply connected to the stator circuit is based on the reactive power component of the machine, and it is calculated as DC supply = $3.678 \times 2.784 = 10.2$ V. Alternatively, the DC supply can be estimated from DC-link voltage source characteristics as shown in Figure 5b. The point of changeover switch action (i.e., stator connection from SC to DC supply) is assessed based on current stabilization characteristics. The rotor speed at which the transfer switch is operated from the stator short-circuit to the fixed dc supply is 53% of the synchronous speed.

To demonstrate energy-efficient starting, a 2.2 kW DFAM is modelled and simulated in MATLAB/Simulink software. The sampling time is selected as 500 μ s and parameters of 2.2 kW DFAM are presented in Table A1. The simulation test results and comparison are shown in Figure 7. The stator windings are switched from a short circuit to the dc supply at 2.65 s. At the same time, the rotor connections remain the same as the conventional V/f start-up strategy.

Figure 7a compares speed characteristics between conventional and proposed start-up methods. The proposed method rotates at synchronous speed after injecting DC supply to the stator circuit. It shows that the slip losses are negligible when the machine operates at synchronous speed. Meanwhile, the speed of the machine is increased due to the elimination of slip with a slight oscillation. Since the DFAM is started with no-load, this oscillation will not affect the performance of the system. During conventional smooth starting (at 5th s), the machine consumes about 528 watts, (i.e.,) 0.2402 p.u. of real power and 204 watts, (i.e.,) 0.093 p.u. of real power in the two methods, respectively, as shown in Figure 7b of the system. In proposed method (Figure 7c), the three stator windings are carries 1.125 A (0.25 p.u.), 0.562 A (0.125 p.u.), -1.68 A (-0.375 p.u.) per phase (RMS values), respectively. Also, it is observed that the maximum transient current (phase C) produced at the stator circuit during DC injection to stator winding is -1.7325 A (-0.385 p.u.).

The power factor of the conventional start-up method is 0.46 lagging, which means 0.4025 p.u. of reactive power is consumed. In the case of the energy-efficient start-up strategy, the reactive power consumption is reduced to nearly zero by injecting an external DC supply. Hence, the power factor reaches unity, shown in Figure 7d. When applying DC injection to the stator circuit, both the reactive and torque component current produces small transients of about 5.46 A (0.728 p.u.) and the reactive component current becomes nearly zero, the torque component increases to 1.69 A (0.22 p.u.), as shown in Figure 7f.

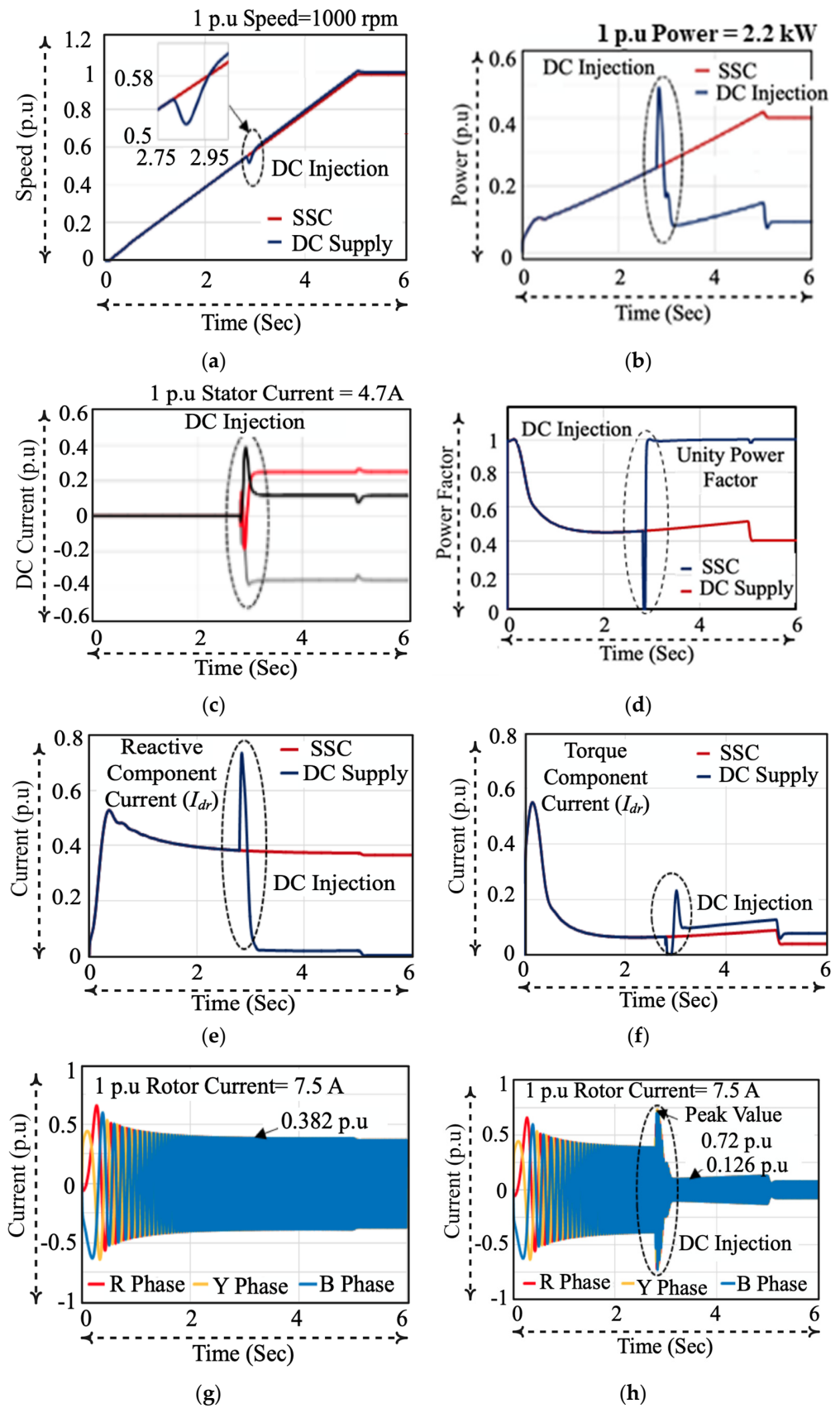


Figure 7. Simulation results of 2.2 kW DFAM during start-up (a) Speed, (b) Power, (c) Stator current, (d) Power factor, (e) Reactive component current, (f) Torque component current, (g) Rotor current—conventional, (h) Rotor current—proposed.

Figure 7g,h shows the rotor currents (Phases R, Y, B) of the conventional and proposed start-up method, respectively. In conventional starting, the rotor current reaches 4.85 A (0.65 p.u.) and is maintained at 2.85 A (0.38 p.u.). In the case of the proposed method, it follows the same pattern until the DC injection. Once the DC supply is injected, the current level is reduced from 0.382 p.u. to 0.126 p.u. with a transient of 0.72 p.u. The simulation results show that the rotor and stator current of the DFAM during the transition period (SC to DC supply) is below the rated current and does not produce any harmful effects on the machine.

4.2. Experimental Results of 2.2 kW DFAM

In the laboratory, the 2.2 kW DFAM is started with the proposed energy-efficient DC injection strategy and the laboratory test results (speed, power, and input current) are compared with the conventional starting method. With the energy-efficient start-up strategy, the stator side windings are switched to the low voltage dc supply at 44% of synchronous speed, and the rotor connections remain the same as the conventional V/f start-up strategy. The duration for smooth starting is selected as 96 s and the stator side windings are switched from the short circuit to the dc supply after 40 s. The DC supply (10.2 volts) is applied to the stator circuit which is similar to the simulation tests and the test results are shown in Figure 8.

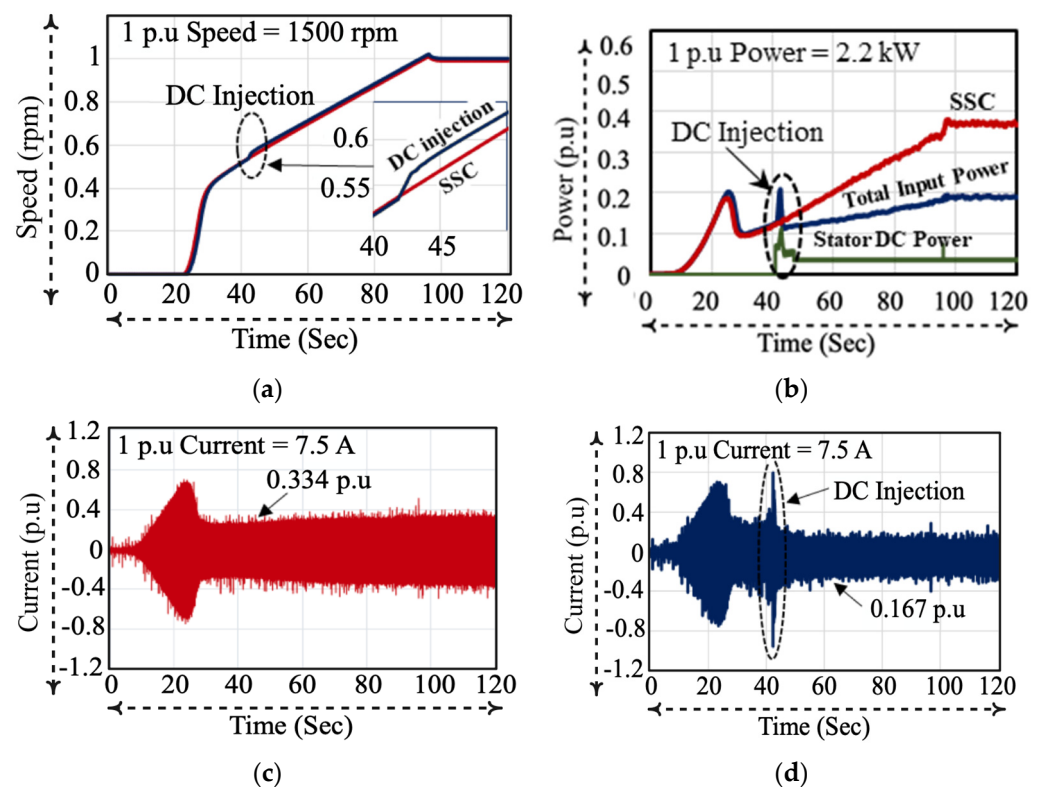


Figure 8. Experimental results of 2.2 kW DFAM during start-up, (a) Speed, (b) Power, (c) Rotor current—Conventional, (d) Rotor current—Proposed.

In the proposed method, the machine rotates at synchronous speed after injecting the DC supply to the stator circuit which eliminates the slip losses. During DC injection, the machine speed is increased after a slight oscillation. Since the DFAM is started with no-load, this oscillation does not affect the performance of the system. Similarly, and importantly, the total power consumption of energy efficient starting is reduced by 26.1% from the conventional SSC start-up. The DFAM under the conventional method consumes about 858 VA (0.39 p.u.) of apparent power. By adopting the proposed strategy, the total power reaches up to 440 VA (0.2 p.u.), shown in Figure 8b. In conventional starting, the rotor current reaches 0.931 p.u. (6.98 A) initially, once the machine begins the acceleration, then

the current stabilizes at 0.334 p.u. (2.51 A) during starting, shown in Figure 8b. In the proposed energy efficient start-up method, the current profile is similar to SSC start-up until the DC voltage is injected. Once the DC supply is injected, the rotor current decreases from 0.33 p.u. (2.47 A) to 0.167 p.u. (1.253 A) with a minimum switching transient. During the switch over point, rotor phase currents oscillations are observed, and phase A carries 1.125 A (0.25 p.u.), phase B carries 0.5625 A (0.125 p.u.) and phase C carries -1.6875 A (-0.375 p.u.). Also, it is observed that the maximum transient current (phase C) produced at the rotor circuit during DC injection to the stator winding is -1.6875 A (-0.375 p.u.), shown in Figure 8d. Experimental results prove that the machine consumes 0.01534 kW-h of energy during conventional start-up, whereas the proposed start-up strategy consumes only 0.00977 kW-h.

5. Smooth Starting of 250 MW Pump Turbine at 1000 MW Tehri PSP—A Case Study

This section analyzes the developed energy-efficient start-up strategy on a 250 MW DFAM based pump-turbine from an economic perspective. In India at the Tehri dam, a DFAM based variable speed pumped storage power plant is under construction, which we'll use for reference. In India at Tehri dam, DFAM based variable speed pumped storage power plant has a capacity of 1000 MW ($250 \text{ MW} \times 4$ units). The Tehri PSP is operated to recycle the discharged water from the lower reservoir, called the "Koteshwar dam". It consists of four units of DFAM-based reversible pump turbines with a capacity of 250 MW each. This plant is being constructed underground on the left bank of the Bhagirathi River. The main feature of this PSP is head variation, which is about 90 m bands. The water system has 3 locations where valves/gates are located. At the intake, a sluice gate is provided followed by a butterfly valve at penstock. Right at the entry of the spiral casing, the main inlet valve (MIV) is provided. All control and protection related sequences make use of MIV. Other valves are used to facilitate maintenance activities of the water conductor system. Speed variation of DFAM is ± 10 percent of the rated speed (230.77 rpm) and the rating of the power converter is about 10% of the machine rating of 250 MW (Figure 9).

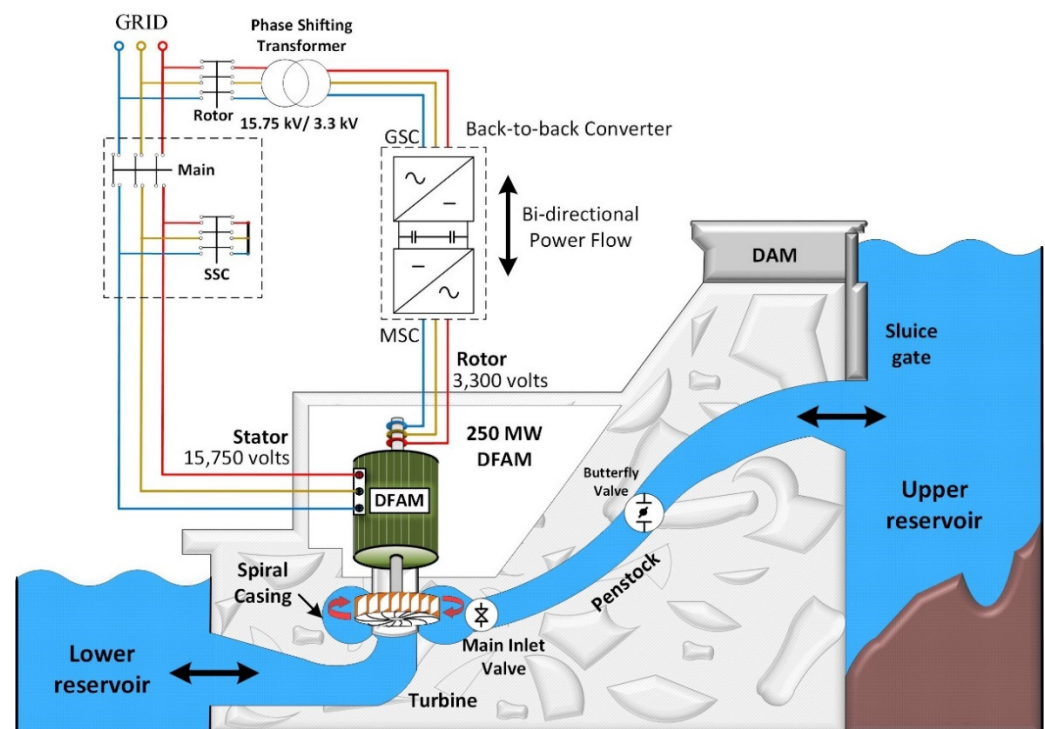


Figure 9. Depiction of 250 MW variable speed pumped hydroelectric unit.

Figure 10 shows the operational sequence of PSPP from generation to pumping. The machine speed is reduced to a standstill and starts back in the reverse direction to transition to the pumping mode from the generation mode. During starting, the energy-efficient start-up sequence is adopted. Implementation of the proposed method in the pumped storage hydropower plant involves the following steps:

- *Step 1:* The stator circuit of the machine is shorted (the main circuit breaker is opened, and SSC is closed), and the rotor is energized with V/f control by machine side converters (MSC). During smooth starting, starting current should not exceed the acceptable limit and maintain a constant torque. The flowchart in Figure 10 indicates the starting sequences.
- The rotor is energized using variable voltage variable frequency ramp supply with short-circuited stator winding for initiating start-up.
- *Step 2:* Stator windings terminals are switched from SSC to the DC supply once the machine attains 25 percent of its rated speed, and is continued up to rated speed (approximately at 70 s from starting). Once DC supply is injected, the reactive power producing current reduces to a minimum value (0.009) p.u. whereas, the torque producing current remains the same. The slip of the machine becomes zero during DC injection which eliminates the slip losses. These factors reduce the overall energy consumption of machines during start-up.
- *Step 3:* Stator windings are switched over to the grid supply once the rotor reaches its rated speed and the gate valve is opened.

To demonstrate the energy efficient starting, a 250 MW DFAM is modelled and simulated in MATLAB/Simulink software and the structure is executed based on the starting sequence given in Figure 10. The switching frequency of the rotor side converter is selected as 300 Hz; the DC-link voltage of the 3-level back-to-back voltage source converter is maintained at 5000 V by grid side converter with the switching frequencies of 500 Hz. The sampling time is selected as 500 μ s and parameters of 250 MW DFAM are given in Table A1.

The duration for smooth starting is selected as 250 s for starting, and boost voltage and frequency ratio are selected as 430 volts and 7 Hz respectively. The fixed DC voltage is selected as 16.8 volts by considering the reactive current component and dc source voltage characteristics (see Figure 5b). The rotor speed at which the changeover switch is operated from stator short-circuited to DC supply is 27% of the synchronous speed. The converter voltage rating is selected by the minimum voltage required during starting of the machine. In the proposed method, the machine rotates at synchronous speed after injecting DC supply to the stator circuit. Thus, the slip losses are zero when the machine operates at synchronous speed. Meanwhile, the speed of the machine is increased due to the elimination of slip with a slight oscillation. Since the DFAM is started with no-load, this oscillation should not affect the system's performance. Likewise, during start-up with SSC, the rotor line voltage ramps from 990 to 3300 volts and consumes power up to 15.48 MVA (max), which includes 9.8 MW of active power and 11.95 MVAR of reactive power, whereas the proposed strategy consumes up to 11.38 MVA (max), shown in Figure 11b. Once after stabilization, the power consumption is reduced to 6.67 MVA and 2.08 MVA for the conventional SSC and the proposed DC injection strategy respectively. In the conventional method, the machine consumes about 0.2896 p.u (3128 A) of reactive component current for magnetization and 0.210 p.u (2268 A) of torque component current for acceleration. Whereas, both reactive and torque component current produces transients of about 0.4742 p.u (5121 A) and when the reactive component current approaches zero, the torque component rises to 0.2554 p.u (2748 A) during DC injection, as shown in Figure 11c,d.

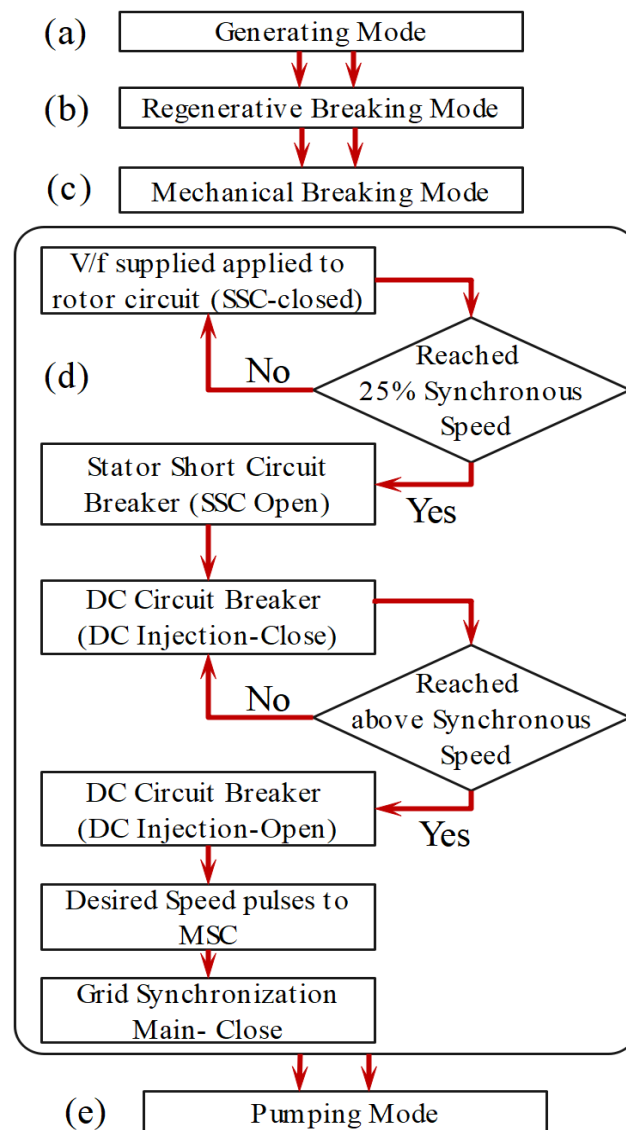


Figure 10. Operation sequence of DFAM from generating mode to pumping mode. (a) generation, (b) regenerative braking, (c) mechanical braking, (d) proposed starting, (e) pumping.

During the short circuit condition on the stator side, Phase A carries 0.308 p.u (3465 A), phase B carries -0.02 p.u (225 A) and phase C carries -0.284 p.u (-3195 A) currents, shown in Figure 11e. Also, it is observed that the maximum transient current (phase A) produces at the stator circuit when DC is injected to stator winding is 0.55 p.u (6188 A), shown in Figure 11f. The simulation results show that the rotor and stator current of the DFAM during the transition period (SSC to DC injection) is below the rated value (10,800 A) and it should not produce any harmful effect on the machine.

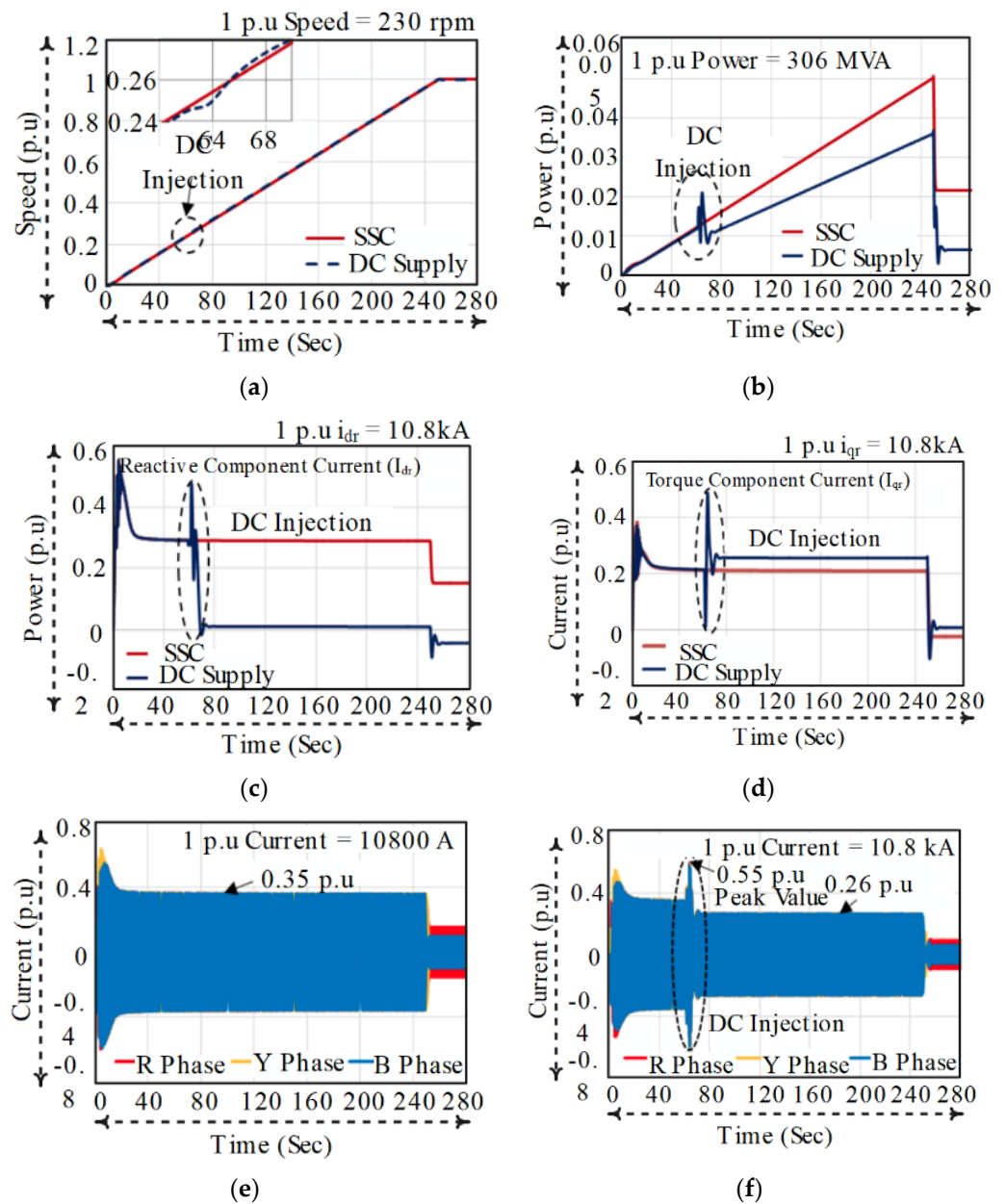


Figure 11. Electrical and mechanical quantities of 250 MW DFAM during V/F start-up, (a) Speed, (b) Power, (c) Reactive component current, (d) Torque component current, (e) Rotor current—Conventional, (f) Rotor current—Proposed.

The energy consumption of DFAM with conventional stator short circuit start-up method and DC injection start-up method are presented in this section. Experimental results ae evidently shows that during conventional start-up, the machine consumes 0.01534 units (kW-h) of energy whereas the proposed start-up strategy consumes only 0.00977 units. The estimation of energy consumption is calculated through the Equations (5)–(7) and the results are tabulated in Table 1. The experimental results evidently prove that there is less transients (0.781 p.u = 5.86 A) during transition period (SSC to DC injection) and also saves about 36.31% energy from conventional stator short circuit based start-up of pump turbine. Similarly, the proposed energy efficient smooth starting method for 250 MW DFAM saves about 35.35% energy from conventional stator short circuit-based start-up of pump turbine.

Table 1. Energy Consumption of DFAM with Conventional Start-up and DC Injection Start-up.

	2.2 kW DFAM		250 MW DFAM	
	Conventional start-up—Stator short circuit			
Zero—rated speed (a)	0.0108 kWh	(0 to 100 s)	537.79 kWh	(0 to 250 s)
Rated speed—synchronization (b)	0.004534 kWh	(100 s to 120 s)	113.37 kWh	(250 s to 310 s)
Total (c = a + b)	0.01534 kWh	(0 to 120 s)	651.16 kWh	(0 to 310 s)
Proposed start-up—DC Excitation				
Zero—switchover speed * (d)	0.00225 kWh	(0 to 43 s)	321.73 kWh	(0 to 66 s)
Switchover *—rated speed (e)	0.00519 kWh	(43 s to 100 s)	321.73 kWh	(66 s to 250 s)
Rated speed—synchronization (f)	0.00233 kWh	(100 s to 120 s)	14.09 kWh	(250 s to 310 s)
Total (g = d + e + f)	0.00977 kWh	(0 to 120 s)	420.96 kWh	(0 to 310 s)
Total energy conserved/unit (c – g)	0.00556 kWh		230.20 kWh	
% Energy saving = $\left(\frac{c-g}{c}\right) \times 100\%$	36.31%		35.35%	

* Switchover speed for 2.2 kW DFAM is 55% and 250 MW DFAM is 27%.

The benefit of this proposed method is estimated for a 250 MW pump-turbine at 1000 MW Tehri PSP. The energy consumption and conservation for each unit of the plant are calculated and presented in Table 2, using the assumption of starting the DFAM with the proposed EC strategy twice per day and 360 days of operation in a year. If the pump-turbine is started twice a day, the financial benefits are approximated as Rs. 5 lakhs/year (at Rs. 3/kWh), or about \$6600 USD/year. The machine' at stator short-circuited and the DC injection strategy was calculated using (5)–(7). If this calculation is extended for all four units, total financial benefits will be estimated as Rs. 20 lakhs/year about \$26,400 USD/year. The cost of the proposed energy efficient start-up system is much lower than this financial benefit and provides a payback period of less than one year.

$$E_s = (E_{SSC} - E_{DC}) \times S_T \quad (5)$$

$$E_{SSC} = \sum_{n=1}^{\infty} \left\{ \frac{(\alpha_{n+1} - \alpha_n)(\beta_{SSC_{n+1}} - \beta_{SSC_n})}{2} \right\} \quad (6)$$

$$E_{DC} = \sum_{n=1}^{\infty} \left\{ \frac{(\alpha_{n+1} - \alpha_n)(\beta_{DC_{n+1}} - \beta_{DC_n})}{2} \right\} \quad (7)$$

where, E_s is total energy saved in kilowatt-hour, E_{SSC} is the total energy consumed during starting with stator short circuit method kilowatt-hour, E_{DC} is the total energy consumed during starting with the proposed starting scheme in kW-hr, S_T is total starting time in hours, n is the number of samples, α is the starting time in hrs., β_{SSC} is the power consumed on stator short circuit method in watts, and β_{DC} is the power consumed on the proposed scheme in kW. From this analysis, it is found that the energy savings during starting of the DFAM-based pump-turbine by adopting the new start-up method is 26.1%, leading to a significant economic benefit.

Table 2. DC Injection Start-Up EC Strategy For 1000 MW (4 × 250 MW) DFAM.

Process	Per Start-Up (kWh)	Start-Up Per Day (kWh) *	Start-Up Per Day (kWh) **
SSC	881.36	1762.72	634,579
DC Injection	651.16	1302.32	468,835
EC/Unit	230.2	460.4	165,744
EC (4 units)	920.8	1841.60	662,976

* 2 times of starting in a day; ** 360 days of operation in a year.

6. Conclusions

This paper has demonstrated the advantages of an energy saving strategy for the starting of a doubly fed asynchronous machine drive. Proposed energy conservation (EC) strategies are developed with minimum possible capital expenditures, downtime, and resource requirement. Practical implementation and analysis of the developed EC strategy on test machines reveal a significant improvement in efficiency and reduction in power consumption during starting. Moreover, the proposed EC start-up strategy is flexible to adapt to existing doubly fed variable speed drive without extensive modification, including hydro and other applications. Also, it is found that low voltage DC injection reduces the vibration of the machine due to the reduction in current magnitude, which is the prime factor of various applications. An economic benefit of a actual 1000 MW variable speed PSP was estimated using publically available data. The test results showed that around 26.1% of energy should be conserved during the starting of this example pump turbine by adopting the new start-up method, leading to a significant economic value.

Author Contributions: All authors contributed equality in each task towards the paper. More specifically: R.R.S.: Conceptualization, Methodology, Writing—original draft. M.B.: Investigation, Formal analysis. U.S.: Software, Validation. M.S.B.: Visualization, Writing—review & editing. S.S.R. Project administration, Data curation. H.A.A.: Software, Visualization. E.R.C.: Resources, project administration, data curation, writing, review and editing. T.S.: Overall coordination. All authors have read and agreed to the published version of the manuscript.

Funding: This research received no external funding.

Institutional Review Board Statement: Not applicable.

Informed Consent Statement: Not applicable.

Data Availability Statement: Not applicable.

Conflicts of Interest: The authors declare no conflict of interest.

Appendix A

Table A1. DFAM (2.2 kW, 4 POLES, 1460 RPM, 50 Hz).

Parameters	2.2 kW	250 MW
Stator voltage	415 V	15,750 V
Stator current	4.7 A	11,250 A
Rotor voltage	185 V	3300 V
Rotor current	7.5 A	11,600 A
Speed	1460 RPM	230.77 RPM
Poles	4 Poles	26 Poles
Stator resistance	3.678 Ω	0.00252 Ω
Rotor resistance	5.26 Ω	0.00104 Ω
Stator inductance	306.82 mH	0.00494 H
Rotor inductance	306.82 mH	0.00507 H
Stator leakage inductance	24.87 mH	0.00038 H
Rotor leakage inductance	24.87 mH	0.00052 H
Magnetizing inductance	281.96 mH	0.00455 H
Moment of inertia	0.014 kgm ²	4.6 $\times 10^6$ kgm ²
Friction of coefficient	0.03 kg m ² /S	0.006 kgm ² /S
Sampling Time	0.001 S	0.0001 S

References

1. Chazarra, M.; Pérez-Díaz, J.I.; García-González, J.; Praus, R. Economic viability of pumped-storage power plants participating in the secondary regulation service. *Appl. Energy* **2018**, *216*, 224–233. [CrossRef]
2. Abdellatif, D.; AbdelHady, R.; Ibrahim, A.M.; El-Zahab, E.A. Conditions for economic competitiveness of pumped storage hydroelectric power plants in Egypt. *Renew. Wind. Water Sol.* **2018**, *5*, 2. [CrossRef]
3. LeDoux, K.; Visser, P.W.; Hulin, J.D.; Nguyen, H. Starting Large Synchronous Motors in Weak Power Systems. *IEEE Trans. Ind. Appl.* **2015**, *51*, 2676–2682. [CrossRef]
4. Joseph, A.; Desingu, K.; Semwal, R.R.; Chelliah, T.R.; Khare, D. Dynamic Performance of Pumping Mode of 250 MW Variable Speed Hydro-Generating Unit Subjected to Power and Control Circuit Faults. *IEEE Trans. Energy Convers.* **2018**, *33*, 430–441. [CrossRef]
5. Kuwabara, T.; Shibuya, A.; Furuta, H.; Kita, E.; Mitsuhashi, K. Design and dynamic response characteristics of 400 MW adjustable speed pumped storage unit for Ohkawachi power station. *IEEE Trans. Energy Convers.* **1996**, *11*, 376–384. [CrossRef]
6. Mitsubishi Electric Corporation, Pumped Storage Power Station with Adjustable Speed Pumped Storage Technology. Available online: <https://openjicareport.jica.go.jp/pdf/12044822.pdf> (accessed on 1 January 2021).
7. Lung, J.; Lu, Y.; Hung, W.; Kao, W. Modeling and Dynamic Simulations of Doubly Fed Adjustable-Speed Pumped Storage Units. *IEEE Trans. Energy Convers.* **2007**, *22*, 250–258. [CrossRef]
8. Koutnik, J. Frades II—Variable speed pumped storage project and its benefit to the electrical grid. In Proceedings of the Renewable Energy Conference, Orlando, FL, USA, 28–30 January 2012. [CrossRef]
9. Kruger, K.; Koutnik, J. Dynamic Simulation of Pump-Storage Power Plants with different variable speed configurations using the Simsen Tool. *Intl. J. Fluid Mach. Syst.* **2009**, *2*, 334–345. [CrossRef]
10. Alstom, Pumped Hydro Storage Plants by Olivier Teller [Power Point Slides]. Available online: http://www.eletronorte.gov.br/opencms/export/sites/eletronorte/seminarioTecnico/apresentacoesTecnicas/Apresentaxo_08_Teller_Asltom_14-11-12_PSP_seminar.pdf (accessed on 1 January 2021).
11. Yuan, X.; Chai, J.; Li, Y. A Converter-Based Starting Method and Speed Control of Doubly Fed Induction Machine with Centrifugal Loads. *IEEE Trans. Ind. Appl.* **2011**, *47*, 1409–1418. [CrossRef]
12. Saiju, R.; Koutnik, J.; Krueger, K. Dynamic analysis of start-up strategies of AC excited Double Fed Induction Machine for pumped storage power plant. In Proceedings of the 13th European Conference on Power Electronics and Applications, Barcelona, Spain, 8–10 September 2009; pp. 1–8.
13. Singh, R.R.; Chelliah, T.R. Energy saving start-up strategy of pumped storage power plant equipped with doubly-fed asynchronous machine. In Proceedings of the 2016 IEEE 1st International Conference on Power Electronics, Intelligent Control and Energy Systems (ICPEICES), Delhi, India, 4–6 July 2016; pp. 1–8.
14. Oliveira, J.; Nied, A.; Pinho Dias, R. Study on Energy Efficiency of Induction Motor Soft-Starting with Torque Control. In *Advances in Motor Torque Control*; Ahmad, M., Ed.; InTech: Hong Kong, China, 2011; pp. 34–46.
15. Li, Y.; Liu, M.; Lau, J.; Zhang, B. A novel method to determine the motor efficiency under variable speed operations and partial load conditions. *Appl. Energy* **2015**, *144*, 234–240. [CrossRef]
16. Zhang, D.; Zhao, H.; Wu, T. The rotor copper and iron loss analysis of inverter-fed induction motor considering rotor slip frequency. In Proceedings of the IEEE Energy Conversion Congress and Exposition (ECCE), Cincinnati, OH, USA, 1–5 October 2017; pp. 2412–2419.
17. Barton, T.H.; Ahmad, V. The measurement and prediction of induction motor stray loss at large slips. *Proc. IEEE-Part C Monogr.* **1957**, *104*, 299–304. [CrossRef]
18. Naidu, N.; Singh, B. Experimental Implementation of a Doubly Fed Induction Generator Used for Voltage Regulation at a Remote Location. *IEEE Trans. Ind. Appl.* **2016**, *52*, 5065–5072. [CrossRef]
19. Reigosa, D.; Briz, F.; Blanco, C.; Guerrero, J. Sensorless Control of Doubly Fed Induction Generators Based on Stator High-Frequency Signal Injection. *IEEE Trans. Ind. Appl.* **2014**, *50*, 3382–3391. [CrossRef]
20. Abad, G.; López, J.; Rodríguez, M.; Marroyo, L.; Iwanski, G. *Dynamic Modeling of the Doubly Fed Induction Machine*; John Wiley & Sons: Hoboken, NJ, USA, 2003; pp. 209–239.
21. Wang, Z.; Wu, B.; Xu, D.; Cheng, M.; Xu, L. DC-Link current ripple mitigation for current-source grid-connected converters under unbalanced grid conditions. *IEEE Trans. Ind. Electron.* **2016**, *63*, 4967–4977. [CrossRef]
22. Bailey, B. The starting of polyphase squirrel-cage motors. *J. Am. Instit. Electri. Eng.* **1923**, *42*, 1172–1181. [CrossRef]
23. Banerjee, A.; Tomovich, M.; Leeb, S.; Kirtley, J. Power converter sizing for a switched doubly fed machine propulsion drive. *IEEE Trans. Ind. Appl.* **2015**, *51*, 248–258. [CrossRef]
24. Bradley, A. Power Flex Adjustable Frequency AC Drive. In *Rockwell Automation Publication REP*. 20A-UM001O-EN-P. 2014, pp. 1–126. Available online: https://literature.rockwellautomation.com/idc/groups/literature/documents/um/22b-um001_en-e.pdf (accessed on 1 January 2021).
25. Banerjee, A.; Chang, A.; Surakitbovorn, K.; Leeb, S.; Kirtley, J. Bumpless automatic transfer for a switched-doubly-fed-machine propulsion drive. *IEEE Trans. Ind. Appl.* **2015**, *51*, 3147–3158. [CrossRef]
26. Hu, W.-t.; Zhou, Y.-j.; Ren, S.-m.; Zhang, H.-y. A new starting method for asynchronous induction motor. In Proceedings of the 2011 IEEE 2nd International Conference on Computing, Control and Industrial Engineering, Wuhan, China, 20–21 August 2011; pp. 341–344.

-
27. Banerjee, A.; Leeb, S.; Kirtley, J. Solid-state transfer switch topologies for a switched doubly fed machine drive. *IEEE Trans. Power Electron.* **2016**, *31*, 5709–5720. [[CrossRef](#)]
 28. Pannatier, Y.; Kawkabani, B.; Nicolet, C.; Schwery, A.; Simond, J. Optimization of the start-up time of a variable speed pump-turbine unit in pumping mode. In Proceedings of the 2012 XXth International Conference on Electrical Machines, Marseille, France, 2–5 September 2012; pp. 2126–2132.